X-ray Diffraction Studies on Supercooled Aqueous Lithium Bromide and Lithium Iodide Solutions

Toshiyuki Takamuku, Motoyuki Yamagami, Hisanobu Wakita, and Toshio Yamaguchi

Department of Chemistry, Faculty of Science, Fukuoka University, Nanakuma, Jonan-ku, Fukuoka 814-80, Japan

Z. Naturforsch. **52a**, 521–527 (1997); received March 13, 1997

X-ray diffraction measurements were performed on liquid $LiBr \cdot 5H_2O$ and $LiI \cdot 5H_2O$ at temperatures from −30 to 25 °C. The total radial distribution functions did show that on supercooling the hydration shell of the halide ions becomes more structured, while that of the lithium ions becomes distorted. The larger the halide ion, the stronger becomes the water-water interaction around halide ions with lowering temperature. However, the distance between the water molecules in the hydration shells of the halide ions depends little on their size. On the basis of the present results, together with those of our previous investigation on $LiCl \cdot 5H_2O$ at temperatures from −135 to 100 °C, the effects of temperature and the size of the halide ions on the structure of the solution are discussed.

Key words: Lithium Bromide, Lithium Iodide, X-ray diffraction, Supercooled temperature, Hydration structure.

1. Introduction

Structural investigations on supercooled and glassy aqueous electrolytes are essential to understand their crystallization, chemical reactions, hydrogen bonding, and ion-hydration. LiCl, LiBr and LiI are very hygroscopic and form highly concentrated aqueous solutions, which are easily supercooled and vitrified. At ambient temperature, many investigations on these solutions have been performed using X-ray [1–7] and neutron [8–16] diffraction, and computer simulation [17–20] methods. These investigations have revealed that (i) the distances of Li^+–O and Li^+–H(D) are 2.0 and 2.6 Å, respectively, with hydration numbers of four to six, depending on the salt concentration, (ii) that the coordination geometry of the water molecules in the first hydration shell of Li^+ is nearly tetrahedral in highly concentrated solutions, (iii) the distance X^-–O(H_2O) is 3.1, 3.3, and 3.6 Å for Cl^-, Br^-, and I^-, respectively, with hydration numbers of about six, (iv) water molecules approach Li^+ with their dipole axis, while the X^- ion with their O–H bond axis. Most structural investigations on the corresponding undercooled solutions were limited to aqueous lithium chloride [21–32]. Kanno et al. [27] have measured Raman spectra of aqueous LiCl, LiBr and LiI solutions in the glassy state. Both neutron diffraction [30] and inelastic scattering [31] measurements have been performed on aqueous LiCl solutions at various salt concentrations by Dupuy and her co-workers. We have investigated aqueous solutions of the compositions $LiCl \cdot 5H_2O$ and $LiCl \cdot 5D_2O$ in the supercooled and glassy state by X-ray and neutron diffraction [33–36].

In the present study we have extended our X-ray diffraction studies on solutions of the composition $LiBr \cdot 5H_2O$ and $LiI \cdot 5H_2O$, in the temperature range from −30 to 25 °C in order to investigate the effect of the halide ions on the structure of such supercooled solutions.

Reprint requests to Prof. T. Yamaguchi,
Fax +8 19 28 65 60 30.
e-mail: yamaguch@SUNSP1.sc.fukuoka-u.ac.jp.

2. Experimental

2.1. Preparation of Sample Solutions

Lithium bromide and lithium iodide (Wako Pure Chemicals, 99.9%) were dried under vacuum at 110 °C for 24 h and then dissolved in distilled water to reach $[H_2O]/[LiX] = 5$. The densities of the sample solutions at 25 °C were measured with a densimeter DMA 35 (ANTON Paar K.G.), and those of the supercooled solutions were obtained by extrapolation from those between 0 and 100 °C given in [37]. The compositions of the sample solutions are given in Table 1.

0932-0784 / 97 / 0600-0521 $ 06.00 © – Verlag der Zeitschrift für Naturforschung, D-72027 Tübingen

Table 1. Concentrations (mol kg^{-1}), densities ϱ (g cm^{-3}) at 25 °C, the stoichiometric volumes V(Å^3) per lithium atom, and water/salt molar ratio.

	LiBr	LiI
Li^+	11.16	11.10
Br^-	11.16	–
I^-	–	11.10
ϱ	1.517	1.753
V	193.6	212.1
$[H_2O]/[LiX]$	4.979	4.997

2.2. X-ray Diffraction Measurements

The X-ray diffraction measurements were carried out with a Rigaku θ-θ type diffractometer using MoKα radiation ($\lambda = 0.7107$ Å). A LiF (200) bent crystal was used for monochromatization of scattered X-rays. The scattering angle (2θ) ranged from 2 to 140°, corresponding to a scattering vector $s\,(=4\pi\lambda^{-1}\sin\theta)$ from 0.31 to 16.6 Å^{-1}. The measurements were repeated twice over the whole angle range. Different slit combinations and step angles were employed, depending on the angle range. 80 000 counts were collected at each angle. Details of the X-ray diffraction measurements were given in [38, 39]. The temperature of the sample solutions was controlled within ± 0.5 K with a temperature control system [40]. Photolysis of iodide ions by the X-rays was prevented by covering the sample cell with aluminum foil.

2.3. Data Treatment

The measured X-ray intensities, $I(s)$, were corrected for background, absorption, and polarization of X-rays and normalized to electron units by the conventional methods [41–44]. The contribution of the incoherent scatterings which reach a scintillation counter, $I_{\mathrm{inco}}(s) = \Phi(s)\sum x_i I_i^{\mathrm{inco}}(s)$, where $\Phi(s)$ is the fraction of the incoherent radiation, x_i the number of atom i in a stoichiometric volume V containing one Li atom, and $I_i^{\mathrm{inco}}(s)$ the Compton scattering factor of atom i, was deduced from the normalized intensities. Correction for the double scattering was made by the method described in [45]. The structure function, $i(s)$, is given by

$$i(s) = I_{\mathrm{coh}}(s) - \sum x_i f_i^2(s), \tag{1}$$

where $f_i(s)$ represents the atomic scattering factor of atom i corrected for the anomalous dispersion. The s-weighted structure function was Fourier transformed into the radial distribution function $D(r)$ as

$$D(r) = 4\pi r^2 \varrho_0 + \frac{2r}{\pi}\int_0^{s_{\max}} s\, i(s)\, M(s) \sin(r s)\, \mathrm{d}s. \tag{2}$$

Here, $\varrho_0\,(=[\sum x_i f_i(0)]^2/V)$ stands for the average scattering density of a sample solution, and $s_{\max}$ is the maximum s-value attained in the measurements ($s_{\max} = 16.6$ Å^{-1}). A modification function $M(s)$ of the form $[\sum x_i f_i^2(0)/\sum x_i f_i^2(s)]\exp(-0.01\, s^2)$ was used for the sample solutions.

A comparison between the experimental structure function and the theoretical one based on a model was made by minimizing an error square sum

$$U = \sum_{s_{\min}}^{s_{\max}} s^2 \{i_{\exp}(s) - i_{\mathrm{calcd}}(s)\}^2. \tag{3}$$

The theoretical intensities $i_{\mathrm{calcd}}(s)$ were calculated by

$$i_{\mathrm{calcd}}(s) = \sum_i \sum_j x_i n_{ij} f_i(s) f_j(s) \frac{\sin(r_{ij} s)}{r_{ij} s} \exp(-b_{ij} s^2)$$
$$- \sum_i \sum_j x_i x_j f_i(s) f_j(s) \frac{4\pi R_j^3}{V} \frac{\sin(R_j s) - R_j s \cos(R_j s)}{(R_j s)^3}$$
$$\cdot \exp(-B_j s^2). \tag{4}$$

The first term on the right-hand side of (4) is related to the short-range interactions characterized by the interatomic distance r_{ij}, the temperature factor b_{ij}, and the number of interactions n_{ij} for an atom pair i–j. The second term arises from the interaction between a spherical hole and the continuum electron distribution beyond this discrete distance. R_j is the radius of the spherical hole around the ith atom and B_j the softness parameter for emergence of the continuum electron distribution.

All treatments of the X-ray diffraction data were carried out with the programs KURVLR [41] and NLPLSQ [46].

3. Results and Discussion

3.1. Total RDFs

The obtained s-weighted structure functions are shown in Figs. 1(a) and 1(b). The corresponding total radial distribution functions (RDFs), in the $D(r) - 4\pi r^2 \varrho_0$ form, are depicted in Figs. 2(a) and 2(b). The first prominent peak in the RDFs, observed at 3.3 and 3.5 Å for the LiBr and LiI solutions, respectively, is mainly assigned to the X^--H_2O interactions in the

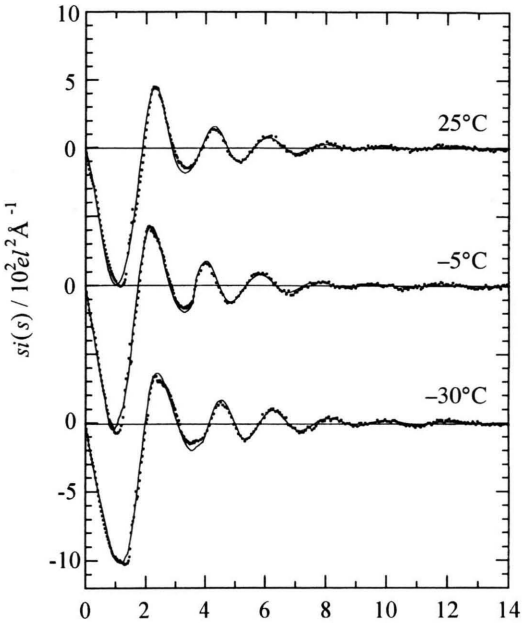

Fig. 1a

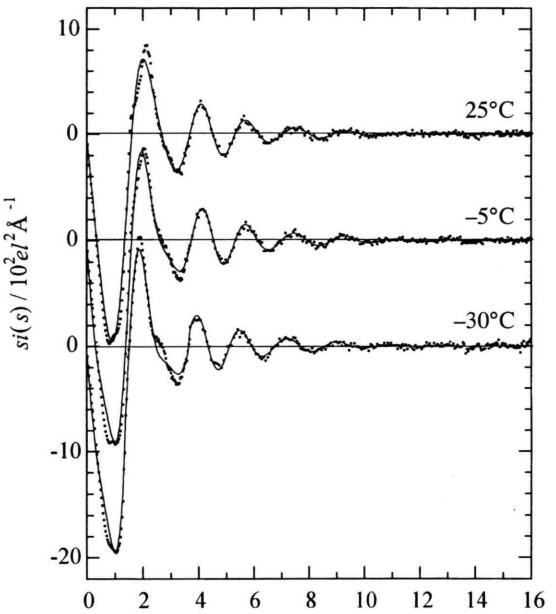

Fig. 1b

Fig. 1. Structure functions $i(s)$ multiplied by s for the aqueous solutions of LiBr (a) and LiI (b) at the three temperatures. Experimental values (dots) and values calculated with the parameters given in Table 2 (solid lines).

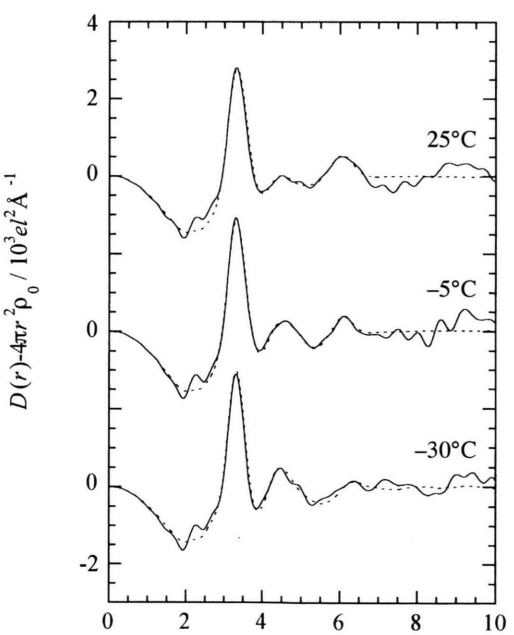

Fig. 2a

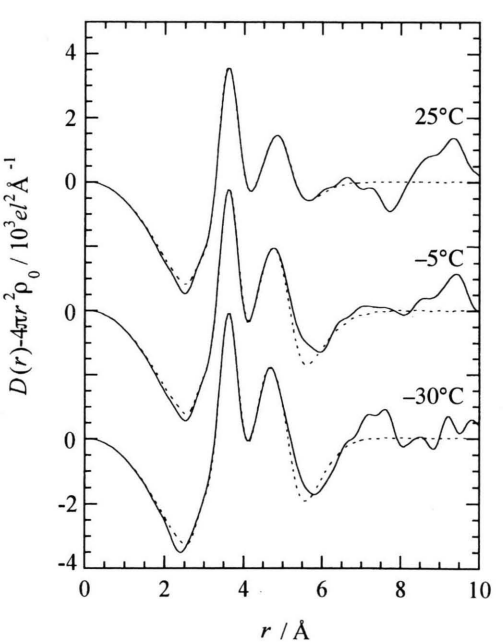

Fig. 2b

Fig. 2. Radial distribution functions (RDFs) in the form of $D(r)-4\pi r^2 \varrho_0$ for the aqueous solutions of LiBr (a) and LiI (b) at the three temperatures: experimental (solid lines) and calculated (dashed lines).

first hydration shell of the halide ions. The difference in the distances reflects difference in the radii of Br^- (1.96 Å) and I^- (2.20 Å). The distances from two other interactions possibly fall in this range. One of them is due to the hydrogen bond H_2O–H_2O interaction, which often appears around 2.8 Å in aqueous electrolyte solutions, and the other is due to the interaction between the water molecules bound to Li^+ in the first hydration shell, described as (Li) $H_2O \cdots H_2O$ hereafter.

Neutron diffraction measurements, recently performed on an aqueous solution with the composition $LiCl \cdot 5D_2O$ [35], have revealed that the Li^+–O distance is 2.02(5) Å and the hydration number of Li^+ about four in the temperature range from −60 to 22 °C. The neutron diffraction technique makes this interaction clearly observable because of the comparable scattering lengths of Li and O atoms. In the present X-ray investigation, however, a peak ascribable to the Li^+–H_2O interaction can hardly be observed because of the weak X-ray scattering power of Li.

In the RDFs for the LiBr and LiI solutions the second peak appears at 4.5–5.0 Å, corresponding to both the $H_2O \cdots H_2O$ interactions in the hydration shell of the halide ions and possible $H_2O \cdots H_2O$ interactions among different hydration shells of the cations and/or anions, the latter being abbreviated as (X) $H_2O \cdots H_2O$ below. In our previous investigation on a supercooled aqueous LiCl solution of similar concentration, the corresponding peak has been observed at 4.5 Å. It is interesting that the position of the second peak is almost independent of the halide ion. Moreover, the peak becomes sharper for the LiI than for the LiBr solution. Furthermore, for the LiBr solution a shoulder on the second peak becomes appreciable around 4.75 Å, which may be assigned to the interaction between Li^+ and Br^-, bridged by one water molecule ($Li^+ \cdots (H_2O) \cdots Br^-$). The corresponding interaction for the LiI solutions is less ambiguous since it may be hidden by the predominant second peak around 4.8 Å.

A broad peak is observed around 6.0 Å for the LiBr solution at 25 °C. According to a molecular dynamics study on a solution with the composition $LiCl \cdot 3H_2O$ at ambient temperature [20], long-range interactions such as $H_2O \cdots H_2O$, $Cl^- \cdots H_2O$, and $Cl^- \cdots Cl^-$ between different hydration shells of chloride ions appear around 6.0 Å. The broad peak at 6.0 Å seen for the present LiBr solution at 25 °C may, thus, be assigned to the long-range interactions, $H_2O \cdots H_2O$, $Br^- \cdots H_2O$, and $Br^- \cdots Br^-$. In subsequent calculations of theoretical curves, this peak was represented only by $H_2O \cdots H_2O$ interactions, to minimize the number of independent variables in the fits. For the LiI solution at 25 °C, the corresponding peak is observed at the slightly longer distance 6.5 Å, but is less pronounced; thus, the peak was not taken into account in the model calculations. For the long-range interactions beyond 6.5 Å an even electron distribution was assumed.

With lowering the temperature from 25 to −30 °C, the first peak at 3.3–3.5 Å, due mainly to the X^-–H_2O interaction, becomes sharper for both solutions. The second peak at 4.5 Å for (X) $H_2O \cdots H_2O$ interactions increases with decreasing temperature. The shoulder around 4.75 and 4.8 Å, assigned to the $Li^+ \cdots (H_2O) \cdots X^-$ interaction increases with lowering temperature. Similar changes in the RDFs with temperature have been observed for the aqueous LiCl solution in [33]. All these findings suggest that the interactions between the water molecules around the halide ions are strengthened with decreasing temperature. On the contrary, the peak around 6.0 and 6.5 Å for the LiBr and LiI solution, respectively, gradually decreases, while the shallow minimum around 7.5 Å gradually evolves when the temperature is lowered to −30 °C. This temperature effect on the long-range interactions is more drastic for the aqueous iodide solution and a new peak appears at about 7.5 Å. These results imply that hydrogen bonds are reinforced and extended to the third neighbors on supercooling, particularly in the solution containing the weakly solvating iodide ions.

3.2. Least-Squares Refinements

To perform a quantitative analysis on the X-ray diffraction data a least squares fitting procedure was applied to the structure function over the range of $0.1 < s/Å^{-1} < 16.6$. In the present calculations, the interatomic distance r, the temperature factor b, and the number of interactions n in Table 2 were treated as variables in (4). With respect to the hydration of Li^+, the hydration number and the Li^+–O distance could not be determined accurately since the corresponding peak is scarcely observable, as described above. Therefore, in the present analysis the Li^+–O distance and the hydration number of Li^+ were fixed to average values ($r = 2.0$ Å, $b = 0.01$ Å^2, and $n = 4$), as in [3, 4,

Table 2. Optimized parameter values of the interactions for the aqueous $LiX \cdot 5H_2O$ solutions at the various temperatures: the interatomic distance r (Å), the temperature factor b (Å^2), and the number of interactions n per lithium ion. The values in parentheses are standard deviations. The parameters without standard deviations were fixed during the calculations. The number of H_2O–H_2O interactions was calculated per one bulk H_2O molecule, assuming that the concentration of bulk water was 10 mol dm^{-3}.

Interaction	Parameter	$LiCl \cdot 5H_2O$[a]						$LiBr \cdot 5H_2O$			$LiI \cdot 5H_2O$		
		−135 °C	−80 °C	−30 °C	25 °C	27 °C	100 °C	−30 °C	−5 °C	25 °C	−30 °C	−5 °C	25 °C
H_2O–H_2O	r	2.8	2.8	2.8	2.8	2.8	2.8	2.8	2.8	2.8	2.8	2.8	2.8
	$10^3 b$	8	8	8	8	8	8	8	8	8	8	8	8
	n	0.8(1)	0.7(1)	0.6(1)	0.4(1)	0.4(1)	0.3(1)	0.5(1)	0.4(1)	0.4(1)	0.4	0.4	0.4
X–H_2O	r	3.13(1)	3.13(1)	3.13(1)	3.13(1)	3.13(1)	3.14(1)	3.31(1)	3.30(1)	3.31(1)	3.54(1)	3.54(1)	3.53(1)
	$10^3 b$	5.8(4)	5.9(4)	7.8(3)	10.2(5)	11.6(6)	12.2(8)	16.0(3)	20.0(4)	22.5(4)	17.0(3)	17.0(4)	20.0(3)
	n	6.6(1)	6.5(1)	6.4(1)	6.1(1)	6.1(1)	6.0(1)	5.6(5)	5.8(5)	5.7(5)	5.6(5)	5.6(5)	5.5(5)
(Li)$H_2O \cdots H_2O$	r	3.37(2)	3.39(2)	3.42(1)	3.46(1)	3.49(1)	3.51(1)	3.48(2)	3.46(2)	3.46(2)	3.46(2)	3.47(2)	3.46(1)
	$10^3 b$	10	10	10	10	10	10	10	10	10	10	10	10
	n	3.5(2)	4.1(3)	4.3(1)	4.5(1)	4.6(1)	5.7(1)	3.0(2)	3.2(1)	3.6(1)	3.1(1)	3.4(1)	3.6(1)
(X)$H_2O \cdots H_2O$	r	4.28(1)	4.30(1)	4.35(1)	4.32(9)	4.31(8)		4.33(1)	4.32(1)	4.35(1)	4.42(4)	4.40(4)	4.38(2)
	$10^3 b$	30	30	30	30	30		30	30	30	30	30	30
	n	10.2(3)	8.1(3)	4.0(2)	0.5(1)	0.5(1)		12.9(1)	10.4(1)	9.1(1)	22.0(3)	20.0(2)	11.5(2)
Li$\cdots H_2O \cdots$X	r	4.75	4.75	4.75	4.75	4.75	4.75	4.85(2)	4.81(2)	4.87(2)	4.80(3)	4.82(3)	4.83(3)
	$10^3 b$	20	20	20	20	20	20	35	35	35	35	35	35
	n	2	2	2	2	2	2	0.9(3)	0.5(2)	0.2(1)	10.2(5)	10.0(5)	6.7(6)
$H_2O \cdots H_2O$	r	6.00(3)	6.03(5)	6.04(2)	5.84(1)	5.90(1)	5.86(2)	6.16(3)	6.07(5)	6.03(2)			
	$10^3 b$	30(25)	20(11)	39(22)	48(15)	49(5)	78(5)	40	35	35			
	n	0.3(1)	0.5(1)	0.8(1)	1.3(1)	1.3(1)	2.2(2)	0.1	0.1	0.1			
X$\cdots H_2O$	r	7.04(2)	7.08(3)	7.16(2)									
	$10^3 b$	76(5)	100(11)	100(7)									
	n	6.1(4)	4.4(6)	4.1(3)									

[a] [33]

6–8]. The Li^+–H_2O contribution to the total structure functions was practically negligible in the present system. The finally optimized values are summarized in Table 2. As seen in Figs. 1 and 2, the theoretical $si(s)$ and RDFs calculated by using the values in Table 2 reproduce well the observed ones with the exception of the long range parts not taken into account in the present analysis. The corresponding parameters for the LiCl solution in the temperature range from −135 to 100 °C, determined in [33], were also given in the Table 2 for comparison.

As shown in Table 2, for the LiBr and LiI solutions, from 25 to −30 °C the distance and number of the X^-–H_2O interactions do not change appreciably: $r_{Br-H_2O} \approx 3.3$ Å, $n_{Br-H_2O} \approx 6$ and $r_{I-H_2O} \approx 3.5$ Å, $n_{I-H_2O} \approx 6$. However, the temperature factor decreases from $b_{Br-H_2O} = 0.0225(4)$ Å^2 and $b_{I-H_2O} = 0.0200(3)$ Å^2 at 25 °C to $b_{Br-H_2O} = 0.0160(3)$ Å^2 and $b_{I-H_2O} = 0.0170(3)$ Å^2 at −30 °C. These results show that the first hydration shell of the halide ions becomes gradually structured with lowering temperature. A similar temperature effect has been found for the LiCl solution; the temperature factor decreased from $b_{Cl-H_2O} = 0.0122(8)$ Å^2 at 100 °C to $b_{Cl-H_2O} = 0.0058(4)$ Å^2 at −135 °C. It is very interesting that the number of (X)$H_2O \cdots H_2O$ interactions between water molecules around the halide ions decreases in the order $I^- > Br^- > Cl^-$, $n = 11.5(2)$, 9.1(1), and 0.5(1), respectively, at ambient temperature in spite of the same hydration number of six for I^-, Br^- and Cl^-. This fact can be explained as follows.

If the coordinated water molecules around the halide ions occupy rigid octahedral sites, the distances of the water–water interaction in the hydration shell are expected to be 4.4, 4.7, and 5.0 Å for Cl^-, Br^- and I^-, respectively, on the basis of the X^-–H_2O distances. As seen in Table 2, however, this is not the case, the distances of the (X)$H_2O \cdots H_2O$ interactions fall into the range 4.32(9)–4.38(2) Å for all halide solutions. Here, it is noteworthy that this value is close to the second neighbour distance in the ice-like structure of water. Thus, we can say that the halide ions are

loosely hydrated by water molecules and do not strongly distort the water–water hydrogen-bond network around them, In fact, even the largest iodide ion is small enough to replace one water molecule in the network.

On the basis of the ionic radii, the electrostatic interaction (hydrogen bond) between the halide ions and water molecules is strengthened in a sequence of $Cl^- > Br^- > I^-$. This is also reflected by thermodynamic parameters of hydration; e.g. the enthalpies of hydration at ambient temperature are $\Delta H^\circ = -362.8$, -331.8, and -291.5 kJ mol^{-1} [47] for Cl^-, Br^- and I^-, respectively. Thus, the chloride ions disturb the hydrogen bond network most among the halide solutions, resulting in the smallest number of $(X)H_2O \cdots H_2O$ interactions at ambient temperature. The number of $(X)H_2O \cdots H_2O$ interactions for Cl^-, Br^- and I^- increases from 0.5(1), 9.1(1), and 11.5(2) at 25 °C to 4.0(2), 12.9(1), and 22.0(3) at -30 °C, respectively, clearly showing that the water–water interactions around the halide ions are gradually reinforced with lowering temperature. These results suggest that the hydrogen bonded network is partially recovered around the halide ions at the supercooling temperatures, in particular, around the iodide ion.

Neutron diffraction experiments on supercooled and glassy lithium chloride solutions [35, 36] have revealed a similar increased ordering in both the first and second hydration shell of Cl^- with lowering temperature. Dupuy and her co-workers have recently performed neutron diffraction measurements using a hydrogen and deuterium substitution technique on aqueous solutions with the compositions $LiCl \cdot 6H_2O$ [32a] and $LiCl \cdot 4H_2O$ [32b] in their liquid, supercooled, and glassy states. They have found that both the HH and OO correlations arising from hydrogen bonds increased in the supercooled and glassy states, and they concluded that the hydrogen bonds are strengthened around the ions in these states. Moreover, Raman spectroscopic data on aqueous glassy LiCl solutions with the composition $LiCl \cdot 8H_2O$ and $LiCl \cdot 10H_2O$ [27] have shown that the shoulder (3000–3300 cm^{-1}) on the low-frequency side of the 3430 cm^{-1} OH stretching vibration of water grows with lowering temperature, suggesting an increase in hydrogen bond strength and partial recovery in hydrogen bonding with decreasing temperature.

The opposite feature is observed in the hydration shell of Li^+. The numbers of $(Li)H_2O \cdots H_2O$ interactions in aqueous LiCl, LiBr and LiI solutions gradually decrease with lowering temperature from 4.5(1), 3.6(1), and 3.6(1) at 25 °C to 4.3(1), 3.0(2), and 3.1(1) at -30 °C, respectively, suggesting a distortion of the lithium-ion hydration shell at the supercooling temperature. The previous neutron scattering data with lithium isotopic substitution for a supercooled solution of $LiCl \cdot 5D_2O$ [30, 35, 36] have also revealed a structural change to a less rigid geometry with lowering temperature. It is very interesting that even the rigid hydration shell of Li^+ is distorted in the supercooled solutions.

These structural changes in the hydration shell with lowering temperature suggest that water molecules tend to locally form hydrogen bonded ordering in the solutions, probably accompanied with solute enriched regions. Our X-ray diffraction data on a 5 *m* LiCl solution at undercooled temperature [36] have clearly shown that a locally ice-like network gradually evolves in the solution with lowering temperature, and finally, hexagonal ice (I_h) is formed below -40 °C, together with the supercooled liquid.

4. Concluding Remarks

The present X-ray diffraction data on aqueous lithium halide solutions have demonstrated that a rigid geometrical arrangement of the water molecules in the first coordination shell around Li^+ is gradually distorted with lowering temperature, whereas hydrogen bonds between the water molecules around halide ions are reinforced at low temperatures. This tendency is remarkably promoted in the aqueous solution containing large halide ions because of the more loose binding of water molecules to the large halide ion. Conventional parameters such as the negative values of the Jones and Dole *B*-factors and the smaller Stokes radii than the crystal ionic ones indicate the weak hydration of Cl^-, Br^- and I^- in aqueous solutions. These halide ions are classified as structure-breaking in the Frank and Wen model. The present X-ray investigations on aqueous lithium halide solutions have shown that at an atomic level the halide ions distort the hydrogen-bonded network in water at ambient temperature to such an extent that the weakly distorted network is easily recovered with lowering temperature. On the contrary, it is interesting

that even the hydration shell of Li^+, known as a structure-making, is gradually distorted in the supercooled aqueous solution. Thus, in the supercooled aqueous solutions water tends to locally form ice-like arrangement with excluding solutes. These conclusions may be a hint to understand the crystallization of electrolytes from aqueous solutions and chemical reactions at undercooling temperature.

Acknowledgements

The present work was partially supported by a Grant-in-Aid for Scientific Research (Nos. 06453029 and 08640656) from the Ministry of Education, Science, Sports and Culture, Japan. All the calculations were performed at the Computer Center of Fukuoka University.

[1] R. M. Lawrence and R. F. Kruh, J. Chem. Phys. **47,** 4758 (1967).
[2] D. L. Wertz, J. Solution Chem. **1,** 489 (1972).
[3] A. H. Narten, F. Vaslow, and H. A. Levy, J. Chem. Phys. **58,** 5017 (1973).
[4] G. Pálinkás, T. Radnai, and F. Hajdu, Z. Naturforsch. **35a,** 107 (1980).
[5] I. Okada, Y. Kitsuno, H.-G. Lee, and H. Ohtaki, Stud. Phys. Theor. Chem. **27,** 81 (1983).
[6] G. Paschina, G. Piccaluga, G. Pinna, and M. Magini, Chem. Phys. Lett **98,** 157 (1983).
[7] A. Musinu, G. Paschina, G. Piccaluga, and M. Magni, J. Chem. Phys. **80,** 2772 (1984).
[8] N. Ohtomo and K. Arakawa, Bull. Chem. Soc. Japan **52,** 2755 (1979).
[9] G. W. Neilson, Chem. Phys. Lett. **68,** 247 (1979).
[10] J. R. Newsome, G. W. Neilson, and J. E. Enderby, J. Phys. C: Solid State Phys. **13,** L923 (1980).
[11] J. E. Enderby and G. W. Neilson, Adv. Phys. **29,** 323 (1980).
[12] J. E. Enferby, Philos. Trans. Roy Soc. London **B290,** 553 (1980).
[13] J. E. Enderby, Pure Appl. Chem. **57,** 1025 (1985).
[14] A. P. Copestake, G. W. Neilson, and J. E. Enderby, J. Phys. C: Solid State Phys. **18,** 4211 (1985).
[15] A. Elarby-Aouizerat, J. F. Jal, P. Chieux, J. M. Letoffe, P. Claudy, and J. Dupuy, J. Non-Cryst. Solids **104,** 203 (1988).
[16] K. Ichikawa and Y. Kameda, J. Phys.: Condens. Matter **1,** 257 (1989).
[17] H. Kistenmacher, H. Popkie, and E. Clementi, J. Chem. Phys. **61,** 799 (1974).
[18] M. Mezei and D. L. Beveridge, J. Chem. Phys. **74,** 6902 (1981).
[19] F. T. Marchese and D. L. Beveridge, J. Amer. Chem. Soc. **106,** 3713 (1984).
[20] K. Tanaka, N. Ogita, Y. Tamura, I. Okada, H. Ohtaki, G. Pálinkás, E. Spohr, and K. Heinzinger, Z. Naturforsch. **42a,** 29 (1987).
[21] A. J. Nozik and M. Kaplan, J. Chem. Phys. **47,** 2960 (1967).
[22] C. A. Angell and E. J. Sare, J. Chem. Phys. **52,** 1058 (1970).
[23] C. T. Moynihan, N. Balitactac, L. Boone, and T. A. Litovitz, J. Chem. Phys. **55,** 3013 (1971).
[24] S.-Y. Hsich, R. W. Gammon, P. B. Macedo, and C. J. Montrose, J. Chem. Phys. **56,** 1663 (1972).
[25] H. Kanno and C. A. Angell, J. Phys. Chem. **81,** 2639 (1977).
[26] C. A. Angell, E. J. Sare, J. Donnella, and D. R. MacFarlane, J. Phys. Chem. **85,** 1461 (1981).
[27] H. Kanno and J. Hiraishi, J. Phys. Chem. **87,** 3664 (1983).
[28] D. Clausse, L. Labln, F. Broto, M. Aguerd, and M. Clausse, J. Phys. Chem. **87,** 4030 (1983).
[29] F. Guillaume, M. Perrot, and W. G. Rothschild, J. Chem. Phys. **83,** 4338 (1983).
[30] J. F. Jal, A. K. Soper, P. Carmona, and J. Dupuy, J. Phys.: Condens. Matter, **3,** 551 (1991).
[31] J. Dupuy, J. F. Jal, P. Chieux, and A. J. Dianoux, J. Mol. Struct. **250,** 315 (1991).
[32] (a) B. Prével, J. F. Jal, J. Dupuy-Philon, and A. K. Soper, J. Chem. Phys. **103,** 1886 (1995). (b) ibid. **103,** 1897 (1995).
[33] K. Yamanaka, M. Yamagami, T. Takamuku, T. Yamaguchi, and H. Wakita, J. Phys. Chem. **97,** 10835 (1993).
[34] M. Yamagami, T. Yamaguchi, and H. Wakita, J. Chem. Phys. **100,** 3122 (1994).
[35] T. Yamaguchi, M. Yamagami, H. Ohzono, K. Yamanaka, and H. Wakita, Physica B, **213/214,** 480 (1995).
[36] T. Yamaguchi, M. Yamagami, H. Wakita, and A. K. Soper, J. Mol. Liq. **65/66,** 91 (1995).
[37] O. Söhnel and P. Novotný, ed., Physical Sciences Data 22, Densities of Aqueous Solutions of Inorganic Substances, Elsevier, New York 1985.
[38] H. Wakita, M. Ichihashi, T. Mibuchi, and I. Masuda, Bull. Chem. Soc. Japan, **55,** 817 (1982).
[39] T. Yamaguchi, G. Johansson, B. Holmgerg, M. Maeda, and H. Ohtaki, Acta Chem. Scand. **A38,** 437 (1984).
[40] T. Takamuku, T. Yamaguchi, and H. Wakita, J. Phys. Chem. **95,** 10098 (1991).
[41] G. Johansson and M. Sandström, Chem. Scr. **4,** 195 (1973).
[42] K. Furukawa, Rep. Progr. Phys. **25,** 395 (1962).
[43] J. Krogh-Moe, Acta Crystallogr. **2,** 951 (1956).
[44] N. Norman, Acta Crystallogr. **10,** 370 (1957).
[45] B. E. Warren and R. L. Mozzi, Acta Crystallogr. **21,** 459 (1966).
[46] T. Yamaguchi, Doctoral Thesis, Tokyo Institute of Technology, 1978.
[47] The Chemical Society of Japan, ed., 4th ed. Kagakubinran Kisohen II, Maruzen, Tokyo 1993.